Avian Sulfhydryl Oxidase Is Not a Metalloenzyme: Adventitious Binding of Divalent Metal Ions to the Enzyme†

Stephen G. Brohawn,‡ Irina Rudik Miksa,§ and Colin Thorpe*,‡

Department of Chemistry and Biochemistry, University of Delaware, Newark, Delaware 19716, and New Bolton Center, Toxicology, Department of Pathobiology, School of Veterinary Medicine, University of Pennsylvania, Kennett Square, Pennsylvania 19348

Received June 4, 2003; Revised Manuscript Received July 24, 2003

ABSTRACT: Metal- and flavin-dependent sulfhydryl oxidases catalyze the generation of disulfide bonds with reduction of oxygen to hydrogen peroxide. The mammalian skin enzyme has been reported to be copper-dependent, but a recent protein sequence shows it belongs to the Quiescin/sulfhydryl oxidase (QSOX) flavoprotein family. This work demonstrates that avian QSOX is not a metalloenzyme, and that copper and zinc ions inhibit the oxidation of reduced pancreatic ribonuclease by the enzyme. Studies with Zn^{2+}, as a redox inactive surrogate for copper, show that one Zn^{2+} binds to four-electron-reduced QSOX by diverting electrons away from the flavin and into two of the three redox active disulfide bridges in the enzyme. The resulting zinc complex is modestly air-stable, reverting to a spectrum of the native protein with a $t_{1/2}$ of 40 min, whereas the four-electron-reduced native QSOX is reoxidized in less than a second under comparable conditions. Using tris(2-carboxyethyl)phosphine hydrochloride (TCEP), an alternate substrate of QSOX that binds Zn^{2+} relatively weakly (unlike dithiothreitol), allows rapid inhibition of oxidase activity to be demonstrated at low micromolar metal levels. Zinc binding was followed by rapid-scanning spectrophotometry. Copper also binds the four-electron-reduced form of QSOX with a visible spectrum suggestive of active site occupancy. In addition to interactions with the reduced enzyme, dialysis experiments show that multiple copper and zinc ions can bind to the oxidized enzyme without the perturbation of the flavin spectrum seen earlier. These data suggest that a reinvestigation of the metal content of skin sulfhydryl oxidases is warranted. The redox-modulated binding of zinc to QSOX is considered in light of evidence for a role of zinc−thiolate interactions in redox signaling and zinc mobilization.

Sulfhydryl oxidases catalyze disulfide bond formation with reduction of molecular oxygen to hydrogen peroxide:

$$2R{-}SH + O_2 \rightarrow R{-}S{-}S{-}R + H_2O_2$$

Two broad classes of flavin- and metal-dependent sulfhydryl oxidases have been described in work from the 1970s (*1*−*6*). Recently, flavoenzymes from avian egg white (*7*), human fibroblasts (*7*, *8*), and rat seminal vesicles (*9*) have been shown to be founding members of a new protein family [the Quiescin/sulfhydryl oxidase (QSOX)[1] family (*4*)]. QSOX enzymes contain an N-terminal redox active thioredoxin domain (*10*, *11*) and an ERV/ALR domain (*12*−*16*) closer to the C-terminus (Figure 1). This latter domain represents a novel FAD binding fold containing a redox active disulfide close to the C-4a position of the isoalloxazine ring (*16*, *17*). A range of experiments with QSOX, and the smaller FAD-linked enzymes ERV1p, ERV2p, and ALR, show that the oxidase activity of the sulfhydryl oxidase resides in the flavin domain. QSOX, and their shorter ERV/ALR forms, have a wide range of proposed roles, including the insertion of disulfide bonds into peptides and proteins traversing the secretory pathway (*4*, *15*, *18*, *19*), the maturation of poxviruses (*20*), the assembly of cytoplasmic Fe−S centers (*21*), and roles as tissue growth factors (*4*, *22*, *23*).

The metal-dependent enzymes are less well understood both enzymatically and biochemically. The first metalloenzyme sulfhydryl oxidase to be purified was the iron-dependent enzyme from bovine skim milk membranes (*2*, *24*, *25*). This membrane-associated protein was shown to oxidize a range of thiols, including reduced ribonuclease and chymotrypsinogen (*24*, *26*). In contrast, sulfhydryl oxidases from kidney and skin have been shown to contain bound copper (*5*, *27*−*33*). The enzyme from skin has received considerable attention from Ogawa, Yamada, and colleagues because of its role in the maturation of the dermal layer, its likely involvement in the formation of hair fibers, and its suggested involvement in pathological processes affecting skin function (*28*−*34*). The bovine skin enzyme was found to contain 0.5 mol of copper per 66 000 kDa subunit when

† This work was supported in part by National Institutes of Health Grant GM 26643 (C.T.) and by a Beckman Scholars Award to S.G.B.

* To whom correspondence should be addressed. Telephone: (302) 831-2689. Fax: (302) 831-6335. E-mail: cthorpe@udel.edu.

‡ University of Delaware.

§ University of Pennsylvania.

[1] Abbreviations: ALR, augmenter of liver regeneration; DTT, dithiothreitol; ERV, protein essential for respiration and viability in yeast; ICP/MS, inductively coupled plasma mass spectroscopy; QSOX, flavin-dependent sulfhydryl oxidases homologous to Quiescin Q6; Trx, thioredoxin; TCEP, tris(2-carboxyethyl)phosphine hydrochloride; HEPES, *N*-(2-hydroxyethyl)piperazine-*N*′-2-ethanesulfonic acid.

10.1021/bi0301385 CCC: $25.00
Published on Web 08/26/2003

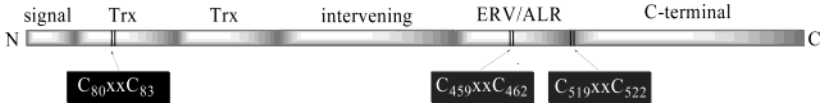

FIGURE 1: Schematic depiction of the domain structure of QSOX. The CxxC motifs are identified in the black boxes with numbering for the avian enzyme. The approximate domain boundaries are as follows: residues 43−144 and 145−255 for the first and second thioredoxin domains, respectively, and residues 419−512 for the ERV/ALR domain.

```
SSOX    32  AARLSVLYSSSDPLTLLDADSVRPTVLGSSSAWAVEFFASWCGHCIAFAP
QSOX    39  AARSRSLYSPSDPLELLGADTAERRLLGSPSAWAVEFFASWCGHCIHFAP

SSOX    82  TWKELANDVKDWRPALNLAVLDCAEETNSAVCREFNIAGFPTVRFFQAFT
QSOX    89  TWRALAEDVREWRPAVMIAALDCADEANQQVCADFGITGFPTLKFFRAFS

SSOX   132  KNGS-GATLPGAGANVQTLRMRLIDALESHRDTWPPACPPLEPAKLNDID
QSOX   139  KKAEDGIRIAHPTATVADLRRAIITNLEQSGDAWPPACPPLEPASAEEVR

SSOX   181  GFFTRNKADYLALVFEREDSYLGREVTLDLSQYHAVAVRRVLNTESDLVN
QSOX   189  SFFHRNTERYLALIFEQSNSFVGREVALDLLQYENVAVRRVLSSEEELVE

SSOX   231  KFGVTDFPSCYLLLRNGSVSRVPVLVESRSFYTSYLRGLPGLTRDAPPTT
QSOX   239  KFGVTTFPSAYLLLRNGSFSRLPVHAEARSFYTYYLQTLSGVTRGSYRLN

SSOX   281  ATPVTADKIAPTVWKFADRSKIYMADLESALHYILRVEVGKFSVLEGQRL
QSOX   289  VTGSAINETRALQPAQADRSKVYVADLESTVHYTLRVEAGRPAVLAGAQL

SSOX   331  VALKKFVAVLAKYFPGQPLVQNFLHSINDWLQKQQKKRIPYSFFKAALDS
QSOX   339  AALKCYVATLAKYFPGRPSVQTFLQSLDSWLRNWTEPELPRSALKEAVKN

SSOX   381  RKED---AVLTEKVNWVGCQGSEPHFRGFPCSLWVLFHFLTVQANRYSEA
QSOX   389  KEDASPAAVLPTNVTWVGCRGSEPHFRGYPCGLWTIFHLLTVQA---AQG

SSOX   428  HPQEPADGQEVLQAMRSYVQFFFGCRDCADHFEQMAAASMHQVRSPSNAI
QSOX   436  GPDEELP-LEVLNTMRCYVKHFFGCQECAQHFEAMAAKSMDQVKSRREAV

SSOX   478  LWLWTSHNRVNARLSGALSEDPHFPKVQWPPRELCSACHNELNGQVPLWD
QSOX   485  LWLWSHHNEVNARLAGGDTEDPQFPKLQWPPPDMCPQCHREERG-VHTWD

SSOX   528  LGATLNFLKAHFSPANIVIDSSASR-HTGRRGSPEATPELLL
QSOX   534  EAAVLSFLKEHFSLGNLYLDHAIPIPMAGEEAAASARLSTAG-
```

FIGURE 2: Alignment of mouse skin sulfhydryl oxidase with avian QSOX. The alignment was generated with Clustal W and is depicted with Boxshade. The N-terminal signal sequences are not shown. The first thioredoxin motif starts at approximately residues 36 and 43 for mouse skin (SSOX) and avian sulfhydryl oxidase, respectively. The three aligned CxxC motifs are denoted with brackets.

the enzyme was purified in the presence of EDTA (*32*). Treatment with excess copper generated a protein containing 1.92 metal ions/subunit with a 1.9-fold increase in activity (*32*).

Surprisingly, a recent sequence of the mouse skin sulfhydryl oxidase (GenBank entry AB044284) from the same laboratory was strikingly homologous to the QSOX family of flavoenzymes (*34*). Figure 2 compares the mammalian (mouse) skin sulfhydryl oxidase (SSOX, top) and avian (chicken) QSOX sequences. Over the full 568 amino acids of the skin sulfhydryl oxidase, there is 51% identity and 26% similarity with the avian enzyme. In particular, the three CxxC motifs (bracketed in Figure 2), within the thioredoxin and ALR/ERV domains, are retained in the skin sequence. Thus, we were concerned that our ongoing mechanistic characterization of this emerging QSOX family of flavin-dependent sulfhydryl oxidases (*3*, *4*, *7*, *18*, *35*−*37*) had missed an essential copper cofactor. Here we report that the currently best-characterized QSOX family member does not require copper for activity and contains very low levels of metals as isolated. Further, the reduced enzyme is inhibited by both copper and zinc. In aggregate, our work suggests that the importance of copper-dependent sulfhydryl oxidases to disulfide bond formation in skin merits reevaluation. Finally, this study shows that metal binding provides unanticipated new tools in the study of the QSOX family of flavoenzymes.

EXPERIMENTAL PROCEDURES

Materials. In general, materials were as described previously (*3*, *18*, *35*, *38*). For metal analysis, stock solutions (1000 ppm) of germanium, molybdenum, and phosphorus in water and arsenic, cadmium, calcium, cobalt, copper, iron, lead, manganese, zinc, scandium, indium, yttrium, and terbium in 4% nitric acid were purchased from SCP Science. The 1577b bovine liver standard reference material was from the National Institute of Standards and Technology (NIST), and bovine adult serum (sterile-filtered) was from Sigma.

All tuning solutions for ICP/MS were from Perkin-Elmer. Threaded Teflon-PFA vessels were purchased from Savillex. Metal free polypropylene sample tubes (Sarstedt) and pipets and pipet tips (Thermo Labsystems) were used with ICP/MS.

General. The purification of egg white sulfhydryl oxidase and other general methods are as described previously (*3*, *38*). The majority of the purification steps of the enzyme, including the first and last steps, utilized 20 mM Tris-HCl buffer containing 0.3 mM EDTA. Samples of the pure enzyme were ultrafiltered against 50 mM HEPES buffer (pH 7.5) without EDTA prior to the studies described here. This buffer was used routinely unless otherwise stated. Where appropriate, buffer solutions were treated with Chelex. To prepare the apoprotein, QSOX (10.2 μM in 2 mL of HEPES buffer) was adjusted to 6 M in guanidine hydrochloride and incubated for 15 min at 20 °C. The solution was distributed into two centrifuge ultrafiltration devices and centrifuged at 4 °C. Each tube was washed twice with 3 M guanidine hydrochloride in HEPES buffer, and the apoprotein was reconstituted with HEPES and pooled.

Metal Analyses. Samples of avian QSOX, and equivalent volumes of buffer alone, were weighed into threaded Teflon-PFA vessels and digested with concentrated HNO_3 (68−71%, w/w) at 90 °C for 12 h. The samples were allowed to cool to room temperature, and 0.4 mL of the digest was mixed with 0.1 mL of a 2.0 ppm internal standard mix, containing Sc, Ge, In, Y, and Tb, followed by 9.5 mL of water. A Perkin-Elmer ELAN 6100 ICP/MS system was optimized according to the manufacturer's recommendations, and performance was evaluated daily using a 0.010 ppm multi-element solution containing Ba, Cd, Ce, Cu, In, Mg, Pb, Rh, and U in 2% nitric acid. Metal binding to QSOX was evaluated by dialysis as follows. Protein (10 μM in 0.3 mL of HEPES/KCl buffer) was dialyzed for 24 h at 4 °C against 550 mL of buffer or 550 mL of buffer containing 1 μM $ZnCl_2$ or $CuSO_4$. Dialyzed samples without protein served as blanks. Samples were recovered for metal analysis as described above.

Spectrophotometry. Static UV−vis spectra were acquired from semimicro or micro cuvettes using an HP8452A diode array spectrophotometer. Anaerobic experiments were performed as described previously (*3*, *35*). Stopped-flow experiments were conducted using a HiTech Scientific SF-61 DX2 instrument in the diode array mode with a 75 W xenon lamp. All spectrophotometric experiments were carried out at 25 °C.

Assays. QSOX was assayed in the oxygen electrode as described previously (*3*, *38*) using either 5 mM DTT or TCEP in HEPES buffer at pH 7.5 and 25 °C. Routinely, the wetted parts of the electrode and cell were rinsed with 10 mM EDTA followed by extensive water washes before each assay. Reduced RNase was prepared and stored as described previously (*18*, *38*). Inhibition experiments that included incubating QSOX, RNase, and metals were performed as follows. Mixtures of reduced RNase (300 μM thiols) and 200 nM QSOX were incubated anaerobically alone, or with either 20 μM $CuCl_2$ or $ZnCl_2$, under a nitrogen atmosphere for 1 h before dilution into an equal volume of reduced RNase (300 μM thiols) in aerobic HEPES buffer. Aliquots (30 μL) were withdrawn at timed intervals and reactions quenched by dilution into 0.12 mL of 0.5 mM DTNB in 50 mM phosphate buffer (pH 7.5, containing 0.3 mM EDTA) prior to analysis for thiol titer.

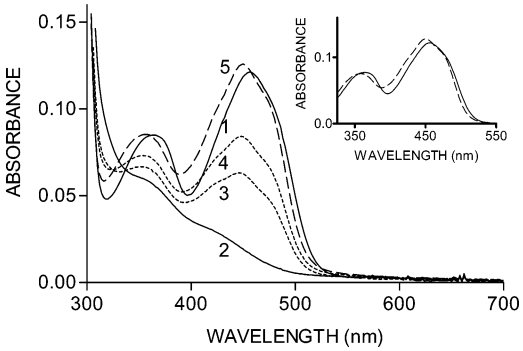

FIGURE 3: Effect of Zn^{2+} on the spectrum of four-electron-reduced QSOX. The enzyme [9.4 μM in 50 mM HEPES buffer (pH 7.5); curve 1] was titrated to the EH_4 state with dithionite (curve 2; see Experimental Procedures) and then mixed anaerobically with 50 μM Zn^{2+} from a sidearm. Curves 3−5 are 60, 90, and 420 s after mixing, respectively. Apparent reoxidation is half-complete in 75 s (not shown). The sample was then opened to air and centrifuged to remove slight turbidity, and the spectrum was remeasured (dashed line in the inset). EDTA (0.5 mM) was then added, and the solid curve in the inset was recorded 20 s after mixing.

Modeling. The coordinates of ERV2p (1JR8) (*16*) were visualized with DS ViewerPro 5.0 from Accelerys Inc. A four-coordinate tetrahedral Zn^{2+} ion was modeled ligated to $C54_{A\ subunit}$, $C109_{B\ subunit}$, $C111_{B\ subunit}$, and either water or $C57_{A\ subunit}$.

RESULTS AND DISCUSSION

Elemental Analysis of Isolated Avian QSOX. Avian QSOX is routinely purified and stored in buffers containing 0.3 mM EDTA (*3*, *38*). For the studies described here, the pure enzyme was then centrifuge-ultrafiltered against HEPES (pH 7.5) without EDTA. ICP/MS (see Experimental Procedures) reveals the presence of 6.60 ± 0.77 atoms of phosphorus per subunit of QSOX (i.e., per FAD). Two of these phosphorus atoms represent the FAD cofactor, and the balance likely reflects additional sites of phosphorylation of this secreted glycoprotein. In line with this observation, other egg white proteins are multiply phosphorylated (*39*). Some disulfide oxidoreductases contain catalytically important selenocysteine residues, e.g., mammalian thioredoxin reductases (*40*−*42*). Avian QSOX is evidently not one of these, since it exhibits insignificant selenium levels. Similarly, the oxidase contains insignificant levels of the following metal/metalloids above buffer blanks: arsenic, cadmium, cobalt, iron, lead, manganese, molybdenum, and zinc. Only copper (at 0.08 ± 0.02 atom per subunit) was significantly above buffer background when the native enzyme was analyzed.

Although zinc levels were undetectable in the native enzyme, we have utilized Zn^{2+} to demonstrate the potential of QSOX to bind transition metals without the attendant complications of redox reactions with the metal itself. Nevertheless, zinc proves to be a powerful modulator of the redox behavior of QSOX as described below. Studies with Cu^{2+} are described later.

Zinc Binding to Four-Electron-Reduced QSOX. Addition of up to 50 μM Zn^{2+} to oxidized QSOX in HEPES buffer (pH 7.5) has no significant effect on the visible spectrum of the flavoprotein (not shown). However, a very different behavior is observed under reducing conditions (Figure 3).

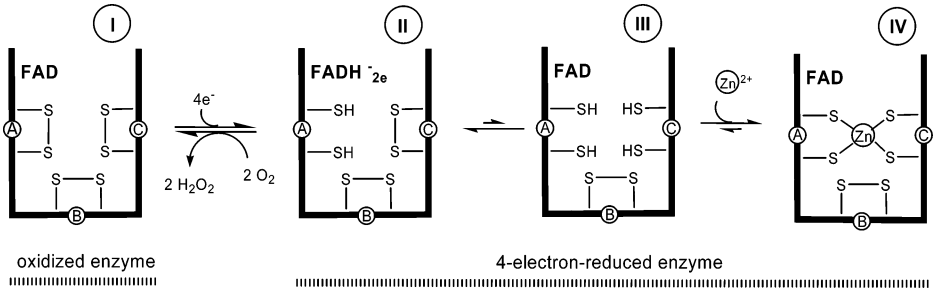

FIGURE 4: Highly schematic depiction of Zn^{2+} binding to the four-electron-reduced form of QSOX. As described in the text, the choice of ligands coordinating the zinc ion is arbitrary.

Curves 1 and 2 represent data for the oxidized and four-electron-reduced enzyme, respectively. Addition of Zn^{2+} from a sidearm to a final concentration of 50 μM effects a marked redistribution of electrons in the four-electron-reduced enzyme. Curves 3 and 4 were recorded 60 and 90 s, respectively, after the addition of this redox inactive metal with the flavin reoxidation complete in 7 min (curve 5).

While the ligands for Zn^{2+} are not yet known, the presence of three CxxC motifs per subunit of QSOX (Figures 1 and 2) and the tight binding of this metal to thiolate ligands make a sulfur-rich coordination environment likely. We have arbitrarily depicted metal binding to four cysteine residues in Figure 4. While this appears to be reasonable, neither this assumption nor the choice of particular cysteine ligands in Figure 4 affects the validity of arguments made later. Thus, while disulfides A and C are depicted as sole contributors in Figure 4, Zn^{2+} binding could involve other pairings and even cysteine residues from each of the three CxxC motifs [with reorganization of the disulfide network (*37*)].

Following completion of the changes under anaerobic conditions (curve 5), the spectrum is 6 nm blue-shifted from the flavin peak of the native enzyme. This suggests a significant change in the environment surrounding the bound isoalloxazine ring. Although the four-electron-reduced native enzyme is reoxidized in <1 s under these conditions [with the intermediacy of the charge-transfer EH_2 state (*3*, *35*)], the zinc-trapped, four-electron-reduced state shows a half-time of 40 min for regain of the oxidized spectrum (not shown). Thus, in addition to the thermodynamic modulation seen in Figure 3, Zn^{2+} binding to the reduced enzyme exerts a marked influence on the kinetic behavior of QSOX. However, 0.5 mM EDTA rapidly reverses complexation, since the spectrum of the oxidized, native, protein appears within the few seconds required for mixing (solid line, inset of Figure 3).

One mode of release of zinc is depicted schematically in Figure 4. Transitory release of zinc (state IV to III), or a change in coordination such that dithiol "A" can successfully access the flavin, would permit the eventual transfer of the four electrons to molecular oxygen. The drastic decrease in zinc affinity on reaction of suitable oxidants with protein thiolate ligands has ample precedent [see later (*43*−*50*)]. With QSOX, oxidative pressure is generated internally through the flavin prosthetic group.

Dithionite Titration of QSOX in the Presence of Zinc. Figure 5 shows a dithionite titration of QSOX in the presence of 50 μM Zn^{2+} at pH 7.5. When the native enzyme is reduced with dithionite, a long wavelength band at 560 nm is observed that is fully formed upon addition of two electrons

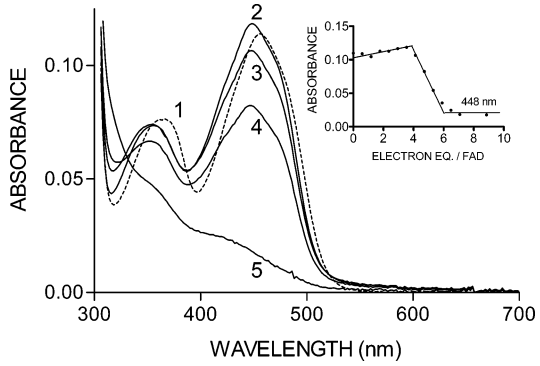

FIGURE 5: Dithionite titration of QSOX in the presence of Zn^{2+}. Enzyme (9.1 μM in HEPES buffer containing 50 μM Zn^{2+}; dashed line, curve 1) was made anaerobic and titrated with dithionite (see Experimental Procedures). Curves 2−5 were recorded 5−10 min after the addition of 3.54, 4.13, 4.72, and 7.08 electrons, respectively. The inset shows the absorbance changes at 448 nm during the titration.

[see later (*3*)]. This conspicuous thiolate to flavin charge-transfer complex is not observed in Figure 5. Instead, the oxidized flavin envelope (dashed, curve 1) blue shifts and intensifies slightly (curve 2, Figure 5) with the addition of a total of four electrons (see the inset). After this phase, introduction of a further two electrons leads to the fully reduced spectrum (curve 5; curves 3 and 4 are intermediate spectra). No significant long wavelength band, attributable to a charge-transfer complex or to a semiquinone species, is evident in this final phase of the titration. No further spectral changes to the enzyme are evident with the further addition of a total of eight electrons (not shown).

Stoichiometry of Zinc Binding to Four-Electron-Reduced QSOX. Figure 6 shows a titration of the four-electron-reduced native enzyme with zinc followed at 450 nm. The four-electron-reduced enzyme was generated via dithionite titration, and a standardized zinc chloride solution was added anaerobically from a second syringe. The incremental absorbance increase at 450 nm progressively slows as 1 equiv is reached, eventually requiring several hours for completion. There are likely two main reasons why zinc binding to the dithionite-reduced enzyme is relatively slow. First, there are multiple zinc binding sites in avian QSOX (see later). Thus, the free metal concentration during a zinc titration is likely to be reduced by this additional binding. Redistribution of zinc to the active site thiols of QSOX might well be slow. More importantly, the equilibrium between forms II and III in Figure 4 lies far in the direction of form II (*3*, *35*). This reduced flavin species has only two, not four, potential thiolate ligands in the active site. The low equilibrium concentration of form III would be expected to significantly

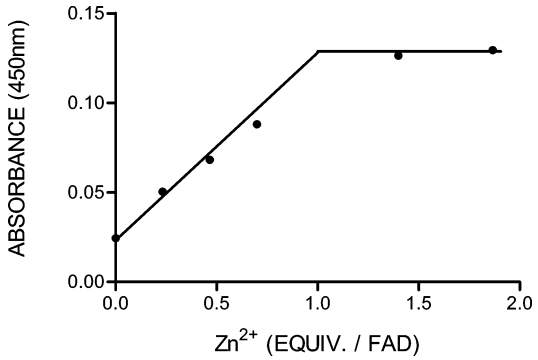

FIGURE 6: Stoichiometry of Zn^{2+} binding to four-electron-reduced QSOX. The four-electron-reduced enzyme (9.9 μM) was prepared by dithionite titration (see Experimental Procedures) and titrated with a solution of zinc chloride. The time taken for the spectral changes to be completed increased markedly throughout the titration. Thus, the last two data points were recorded after overnight incubation to ensure completion.

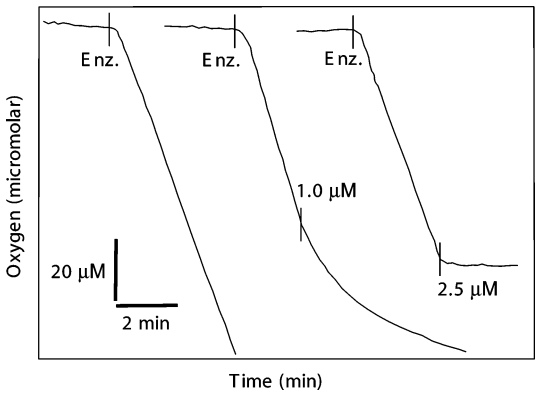

FIGURE 7: Inhibition of QSOX activity by Zn^{2+} measured in the oxygen electrode. Assays in 2 mL of 5 mM TCEP in HEPES buffer (pH 7.5, 25 °C) were initiated by the addition of 100 nM QSOX after the background rate was recorded. Either 1.0 or 2.5 μM Zn^{2+} was added as indicated in the middle and right trace.

slow the capture of the four-electron-reduced enzyme by zinc. However, a reductant that directly reduces one or more of the CxxC motifs of QSOX, rather than the flavin (as in dithionite treatment), might allow a more rapid capture of the enzyme by zinc ion. This is because reducing equivalents do not appear to rapidly equilibrate over the four redox centers in QSOX, and the rate-determining step in catalysis appears to be communication between CxxC motifs and the flavin (*4*, *35*, *37*).

Zinc Binding Can Rapidly Inhibit QSOX Activity. Zn^{2+} concentrations up to 50 μM are not significantly inhibitory when QSOX is assayed with 5 mM DTT under standard conditions (not shown). This is not surprising because DTT strongly coordinates Zn^{2+}, forming monomeric and polymeric complexes (*51*). Thus, we needed an alternate reducing substrate of QSOX that would bind metal more weakly than DTT. Tris(carboxyethyl)phosphine (TCEP) serves this purpose (*52*). This water-soluble phosphine has found wide application as a disulfide reductant in biochemical systems (*53*−*56*) and is a good substrate of QSOX (D. J. Cline, S. G. Brohawn, J. Psathas, and C. Thorpe, unpublished observations). Since preliminary experiments showed that TCEP does not reduce free FAD at a significant rate anaerobically at pH 7.5 (no reaction over several hours; not shown), TCEP must reduce QSOX via one or more of its CxxC motifs.

Figure 7 shows that 2.5 μM Zn^{2+} effects rapid and almost complete inactivation of QSOX when assayed in the oxygen electrode with 5 mM TCEP (see Experimental Procedures). The much slower inactivation with 1 μM Zn^{2+} was puzzling until it was realized that almost all of this nominal concentration of added zinc is rapidly adsorbed to the glass walls and other wetted surfaces of the oxygen electrode assembly. This adsorbed metal is not removed by prolonged rinsing of the cell with deionized water so the subsequent assay would show a steadily decreasing rate as QSOX gathered Zn^{2+} retained in the cell (not shown). The binding of zinc to glass surfaces is well-known, and this complication was avoided by an initial rinse of all contacted components with 10 mM EDTA prior to water washing (see Experimental Procedures). When this EDTA prewash was utilized, oxygen electrode assays with 10 mM TCEP in the absence of zinc exhibited good linearity until low oxygen tensions were reached. This is consistent with the low micromolar K_m for oxygen determined previously (*35*).

It is not the purpose of this paper to evaluate how tightly zinc binds to QSOX. However, binding to the four-electron-reduced enzyme is readily reversed by EDTA (see Figure 3). Precise determination of the K_D for zinc in QSOX is complicated by two factors. First, there are multiple redox states of QSOX with reversible uptake of up to eight electrons (*37*). Even the oxidized enzyme binds multiple metal atoms (see later). Second, zinc binding is rendered air sensitive via oxygen-driven reversal of steps I−IV in Figure 4.

These data show that relatively low concentrations of Zn^{2+} can inactivate QSOX in seconds (Figure 7). Further insight into these events comes from stopped-flow studies following the spectrum of the enzyme during TCEP-driven turnover in the presence and absence of zinc. First, Figure 8A shows the progression of changes in the absence of metal. A lag phase persists at 456 nm before the dissolved oxygen is depleted and the flavin undergoes reduction (see the inset). Qualitatively, TCEP follows the same progression of spectral changes observed with DTT, although the charge-transfer band in the steady state is less pronounced (*35*). Determining the area under the curve in the inset of Figure 8A and relating it to the concentration of oxygen in this experiment (*57*) give a turnover number of 280 min^{-1}. Under these conditions, TCEP reacts undetectably with oxygen in the absence of enzyme (not shown). In the presence of zinc and oxygen-saturated buffer, the flavin chromophore of QSOX does not bleach, but is rapidly converted to the oxidized, metal-bound spectrum with a $t_{1/2}$ of 5 s (Figure 8B). Thus, zinc binding can proceed rapidly without prior reduction of the flavin when reducing equivalents are delivered via one or more of the CxxC motifs. In contrast, when the four-electron-reduced enzyme is preformed, as in Figures 3 and 6, the subsequent binding of zinc to the redox centers occurs slowly.

Zinc Binding Inhibits Oxidation of Reduced RNase. Studies with a more physiologically relevant substrate are described next. QSOX was preincubated anaerobically with reduced RNase (300 μM protein thiols; see Experimental Procedures) in the presence or absence of zinc. The enzyme was then diluted into an aerobic solution containing additional reduced RNase and assayed by the discontinuous DTNB method [see Experimental Procedures (*38*)]. Under these conditions, 10 μM zinc led to a 40% decrease in enzyme activity in the presence of 300 μM reduced RNase thiols. A somewhat

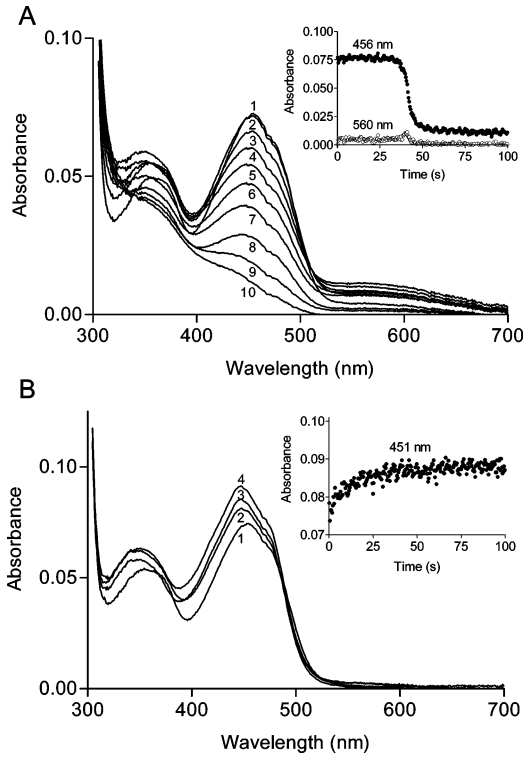

FIGURE 8: Spectral changes accompanying inactivation of QSOX by Zn^{2+} under aerobic conditions. (A) QSOX in buffer saturated with oxygen was mixed with an equal volume of TCEP in the same buffer (pH 7.5, 25 °C) to give final concentrations of 6.5 μM enzyme, 1.2 mM oxygen, and 4.55 mM TCEP. A total of 600 scans over the course of 240 s were recorded with a selection shown in panel A (0.6, 37.4, 39.0, 40.2, 41.0, 41.4, 42.2, 43.4, 47.0, and 59.8 s for curves 1−10, respectively). The inset plots the absorbance change at 456 and 560 nm with time. Panel B shows data from the same experiment performed but including Zn^{2+} in the syringe containing TCEP to give a final concentration of 50 μM metal. Selected spectra are recorded over the course of 100 s (curves 1−4 are at 0.6, 7.8, 34.6, and 76.6 s, respectively).

stronger inhibition (48%) of the oxidase activity is observed by substituting Cu^{2+} for Zn^{2+} in the RNase assays. Unlike zinc, concentrations of Cu^{2+} of up to 10 μM do not significantly inhibit enzyme-mediated oxidation of TCEP in the oxygen electrode. This is probably because TCEP reduces Cu(II) to Cu(I) (*52*, *58*) and may also serve as a coordinating ligand for copper(I) thiolate species (*59*). The next section describes spectrophotometric experiments with copper and QSOX.

Titration Experiments with Copper Binding to QSOX. The addition of 5 equiv of Cu(II) to the oxidized enzyme has no significant effect on the visible spectrum of QSOX (not shown). However, copper has a marked effect during a dithionite titration of avian QSOX. First, for comparison, Figure 9C shows the oxidized and the two-electron-reduced form of the native metal-free enzyme observed during dithionite reduction or photochemical reduction. The long wavelength band centered at 560 nm, extending beyond 700 nm, is characteristic of a thiolate to FAD charge-transfer complex at the EH_2 level (*3*, *60*, *61*). In contrast, reduction in the presence of copper leads to a long wavelength band that accumulates between two and four electrons (Figure 9A,B). This feature has little absorbance beyond 600 nm, in marked contrast to the EH_2 state of the native enzyme (Figure 9C). In addition, a distinct small maximum at 410 nm appears with reduction of the enzyme in the presence of copper.

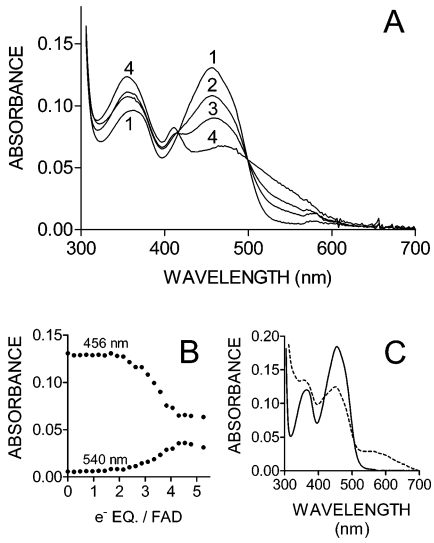

FIGURE 9: Reduction of QSOX in the presence of copper ions. Panel A shows titration of an anaerobic solution of QSOX [10.7 μM with 50 μM $CuSO_4$ in 0.8 mL of 50 mM HEPES buffer (pH 7.5) containing 100 mM KCl; curve 1] with 3.11, 3.58, and 4.54 electron equivalents of dithionite (curves 2−4), respectively. Intermediate traces are omitted for clarity. Panel B shows absorbance values at 456 and 540 nm as a function of the number of electrons per flavin delivered during the titration. For comparison, panel C shows the oxidized and two-electron-reduced enzyme formed during the reduction of QSOX in the absence of Cu^{2+}.

These spectral changes are similar in a number of aspects to those observed upon addition of copper(I) species to oxidized free flavin in acetone and water (*62*). A crystal structure of a $Cu(I)(flavin)_2$ complex reveals coordination between C(4)O and N5 of each of two oxidized isoalloxazine rings, yielding green-black crystals (*63*). The data in Figure 9 are consistent with a close approach between the copper center and the flavin in QSOX.

While the three-dimensional structure of QSOX has yet to be determined, the crystal structure of ERV2p (*16*) provides an attractive putative metal site for zinc or copper ions. The flow of reducing equivalents in ERV2p is believed to proceed via interchange between two disulfides across the subunit interface of the dimer:

$$\text{(di)thiol substrate} \rightarrow (\text{C109/111})_{\text{B subunit}} \rightarrow (\text{C54/57})_{\text{A subunit}} \rightarrow \text{FAD} \rightarrow \text{oxygen}$$

The distal redox active CxC motif (C109/111) is located at the flexible C-terminus of ERV2p and, upon reduction, can form a mixed disulfide with C54 of the CxxC disulfide of the other subunit (*16*). This later motif interacts directly with the flavin in ERV2p (*16*). QSOX has the same complement of redox active disulfides in its ERV domain; however, it substitutes the CxC domain with a comparably placed CxxC disulfide (*4*, *16*, *37*). As described in this work, four-electron reduction of QSOX generates a metal site for zinc or copper (Figure 4). Reducing both disulfides of ERV2p *in silico* (see Experimental Procedures) shows that a zinc ion could be coordinated by cysteine residues $C54_A$, $C109_B$, and $C111_B$ and a solvent water molecule or, conceivably, $C57_A$. Obviously, these modeling exercises should be treated with considerable caution, but they do suggest that a metal site could be created from both redox active disulfide moieties in the ERV domain of QSOX. In addition to these two

disulfides, QSOX contributes a third pair of candidate ligands from the CxxC motif of the N-terminal thioredoxin domain (Figure 2). Obviously, a crystal structure of QSOX is needed to begin the search for the new metal site created upon reduction of the enzyme.

Redox Modulation of Zinc Binding. The redox-dependent ligation of zinc described in this paper has ample precedent, and shows interesting parallels to certain redox switching effects *in vivo*. For example, a zinc ion is bound tightly to a cluster of four cysteine residues in the C-terminal region of the prokaryotic heat shock protein Hsp33 (*48*−*50*). Oxidative stress raises the cytosolic redox poise, and leads to the oxidation of the metal thiolate cluster, resulting in the generation of two intramolecular disulfides, the extrusion of zinc, and the activation of Hsp33 (*48*−*50*). A number of the biological effects of zinc-finger and ring-finger proteins are modulated via oxidation of cysteine residues and expulsion of metal (*47*, *64*−*68*). Cellulose synthase contains an N-terminal cytoplasmic zinc ring-finger domain which, upon oxidation, leads to higher-order rosette structures mediated via formation of intermolecular disulfides (*69*). In addition, metallothionein has been shown by Maret, Vallee, and others to unload zinc on conversion of cysteine thiolate ligands to disulfides using oxidized glutathione, hydrogen peroxide, nitric oxide, and other oxidants (*45*, *70*−*72*). In all these examples, an external reagent is the immediate oxidant for the zinc-bound species. In QSOX, oxidative pressure comes from the direct redox connection between flavin and disulfide moieties of the enzyme. There is one example in the older literature of relevance to the present work. Zinc binding to lipoamide dehydrogenase was first noted in 1966 and suggested to involve the cysteines generated upon reduction of the (single) catalytic disulfide of this enzyme (*73*−*75*). This observation has recently been rediscovered and extended by Gazaryan *et al*. (*76*), who showed that submicromolar levels of zinc inhibit the NADH/lipoamide activity of this flavoenzyme. Correspondingly, the zinc-treated enzyme exhibits enhanced oxidase activity leading to the potential for enhanced generation of reactive oxygen species *in vivo* (*76*). Whether metal binding to the cluster of cysteines near the flavin in QSOX, or to equivalent residues in the smaller oxidases ERV1p/ALR and ERV2p, plays any physiological role awaits further study.

Metal Binding to Oxidized QSOX. The data presented above show that both zinc and copper bind to reduced QSOX and modulate both redox equilibria and enzyme activity. However, anaerobic conditions are only likely at the very earliest stages of an enzyme purification procedure (when homogenization releases endogenous substrates and their cognate oxidases). For this reason, we investigated whether QSOX could bind zinc or copper ions under aerobic conditions. First, QSOX was dialyzed against HEPES buffer (pH 7.5) containing 100 mM KCl in the presence or absence of 1 μM copper or zinc (see Experimental Procedures). After correction for buffer blanks, 4.9 atoms of copper or 2.9 atoms of zinc were bound per flavin (per subunit QSOX). Since loss of flavin sometimes accompanies flavoprotein purification (see later), we also tested metal binding to apo-QSOX. Here, FAD was removed by treating QSOX with 6 M guanidine hydrochloride followed by ultrafiltration to remove first free flavin and then denaturant (see Experimental Procedures). Under the same conditions as holo-QSOX, the apoprotein bound 4.5 atoms of copper or 4.2 atoms of zinc per subunit. Clearly, at the reasonable ionic strength of the buffer system used here (>0.1 M), both holo and apo forms of avian QSOX bind metals at sites other than those made available upon four-electron reduction of the enzyme. These additional sites might lead to the erroneous classification of QSOX as a metalloenzyme.

Avian QSOX Is Not a Metalloenzyme. The data presented here definitively show that avian QSOX does not require metal ions for sulfhydryl oxidase activity. Our study also suggests that a reexamination of the mouse skin sulfhydryl oxidase (*27*−*31*, *33*, *77*, *78*) is warranted. The paper describing the cloning and sequencing of the mouse skin enzyme (*34*) draws attention to its similarity with other members of the QSOX family, but makes no mention of its earlier characterization as a copper-dependent oxidase. A brief mention of these prior studies is relevant here. The initial purification of the skin enzyme in 1980 described a lack of yellow color as evidence of the absence of flavin (*28*). However, it is uncertain whether sufficiently concentrated solutions were available to reliably make this inference in the absence of flavin analyses. For example, the final pure oxidase, after a gel-filtration step, showed a concentration of 70 μg of protein/mL. A 66 kDa flavoprotein at this concentration would exhibit an absorbance of 0.01 at 450 nm. Such absorbance values are below the usual limits of visual detection at 450 nm in a 1 cm path length, and would be even lower if loss of flavin accompanied purification. Two other issues are of note. First, the original report of the purification of the rat skin enzyme describes a single band on SDS−PAGE with a molecular mass of 66 kDa. This is exactly the same subunit size reported for mouse seminal vesicle QSOX (*9*). A human skin sulfhydryl oxidase has been independently reported to have a comparable molecular mass of 65 kDa (*79*), although its complement of prosthetic groups was not examined. Second, both the rat skin oxidase (*28*) and the mouse seminal vesicle QSOX (*9*) exhibit a similar catalytic preference, with the highest activity with DTT and comparatively low activity with reduced glutathione (at 0.17 mM thiol). However, the two enzyme preparations differ markedly in turnover number. Using the data of Takamori *et al*. (*28*), the turnover number of the skin oxidase is ∼100 DTT molecules oxidized per minute per mole of enzyme. This turnover number is much lower than the value of 62 000 min^{-1} reported for the mouse seminal vesicle enzyme for the same substrate (*1*). If this difference reflects a preponderance of apoprotein in the skin oxidase preparation, then added copper might be bound in considerable excess over residual flavin (see above). This copper might then be released upon incubation of DTT and catalyze nonenzymatic (*80*−*82*) thiol oxidation. Finally, immunohistochemical characterization of human skin using a QSOX peptide antibody showed strong staining of the epidermis (personal communication from D. L. Coppock and ref *83*). In summary, the conclusion that skin sulfhydryl oxidases are copper-dependent catalysts should be treated with caution. Monitoring purification profiles, from crude homogenates to pure preparations, using ICP-MS, flavin analyses, QSOX-specific antibody, and enzymatic activity should address the number, and type, of sulfhydryl oxidases that can be detected in mammalian skin.

ACKNOWLEDGMENT

We thank Drs. Karen Hoober and Sonali Raje for gifts of avian sulfhydryl oxidase and Drs. Donald Coppock, Charles Riordan, and Wolfgang Maret for helpful discussions.

REFERENCES

1. Ostrowski, M. C., and Kistler, W. S. (1980) Properties of a flavoprotein sulfhydryl oxidase from rat seminal vesicle secretion, *Biochemistry 19*, 2639−2645.
2. Janolino, V. G., and Swaisgood, H. E. (1975) Isolation and characterization of sulfhydryl oxidase from bovine milk, *J. Biol. Chem. 250*, 2532−2538.
3. Hoober, K. L., Joneja, B., White, H. B., III, and Thorpe, C. (1996) A Sulfhydryl Oxidase from Chicken Egg White, *J. Biol. Chem. 271*, 30510−30516.
4. Thorpe, C., Hoober, K., Raje, S., Glynn, N., Burnside, J., Turi, G., and Coppock, D. (2002) Sulfhydryl oxidases: emerging catalysts of protein disulfide bond formation in eukaryotes, *Arch. Biochem. Biophys. 405*, 1−12.
5. Lash, L. H., and Jones, D. P. (1983) Characterization of the membrane-associated thiol oxidase activity of rat small-intestinal epithelium, *Arch. Biochem. Biophys. 225*, 344−352.
6. de la Motte, R. S., and Wagner, F. W. (1987) *Aspergillus niger* sulfhydryl oxidase, *Biochemistry 26*, 7363−7371.
7. Hoober, K. L., Glynn, N. M., Burnside, J., Coppock, D. L., and Thorpe, C. (1999) Homology between egg white sulfhydryl oxidase and quiescin Q6 defines a new class of flavin-linked sulfhydryl oxidases, *J. Biol. Chem. 274*, 31759−31762.
8. Coppock, D. L., Cina-Poppe, D., and Gilleran, S. (1998) The Quiescin Q6 gene (QSCN6) is a fusion of two ancient gene families: thioredoxin and ERV1, *Genomics 54*, 460−468.
9. Benayoun, B., Esnard-Fève, A., Castella, S., Courty, Y., and Esnard, F. (2001) Rat seminal vesicle FAD-dependent sulfhydryl oxidase: biochemical characterization and molecular cloning of a member of the new sulfhydryl oxidase/quiescin Q6 gene family, *J. Biol. Chem. 276*, 13830−13837.
10. Powis, G., and Montfort, W. R. (2001) Properties and biological activities of thioredoxins, *Annu. Rev. Biophys. Biomol. Struct. 30*, 421−455.
11. Holmgren, A. (1995) Thioredoxin structure and mechanism: conformational changes on oxidation of the active-site sulfhydryls to a disulfide, *Structure 3*, 239−243.
12. Lisowsky, T. (1992) Dual function of a new nuclear gene for oxidative phosphorylation and vegetative growth in yeast, *Mol. Gen. Genet. 232*, 58−64.
13. Lee, J., Hofhaus, G., and Lisowsky, T. (2000) Erv1p from *Saccharomyces cerevisiae* is a FAD-linked sulfhydryl oxidase, *FEBS Lett. 477* (1−2), 62−66.
14. Lisowsky, T., Lee, J. E., Polimeno, L., Francavilla, A., and Hofhaus, G. (2001) Mammalian augmenter of liver regeneration protein is a sulfhydryl oxidase, *Dig. Liver Dis. 33*, 173−180.
15. Gerber, J., Muhlenhoff, U., Hofhaus, G., Lill, R., and Lisowsky, T. (2001) Yeast ERV2p is the first microsomal FAD-linked sulfhydryl oxidase of the Erv1p/Alrp protein family, *J. Biol. Chem. 276*, 23486−23491.
16. Gross, E., Sevier, C. S., Vala, A., Kaiser, C. A., and Fass, D. (2002) A new FAD-binding fold and intersubunit disulfide shuttle in the thiol oxidase Erv2p, *Nat. Struct. Biol. 9*, 61−67.
17. Wu, C. K., Dailey, T. A., Dailey, H. A., Wang, B. C., and Rose, J. P. (2003) The crystal structure of augmenter of liver regeneration: A mammalian FAD-dependent sulfhydryl oxidase, *Protein Sci. 12*, 1109−1118.
18. Hoober, K. L., Sheasley, S. S., Gilbert, H. F., and Thorpe, C. (1999) Sulfhydryl oxidase from egg white: a facile catalyst for disulfide bond formation in proteins and peptides, *J. Biol. Chem. 274*, 22147−22150.
19. Sevier, C. S., Cuozzo, J. W., Vala, A., Aslund, F., and Kaiser, C. A. (2001) A flavoprotein oxidase defines a new endoplasmic reticulum pathway for biosynthetic disulphide bond formation, *Nat. Cell Biol. 3*, 874−882.
20. Senkevich, T. G., White, C. L., Koonin, E. V., and Moss, B. (2002) Complete pathway for protein disulfide bond formation encoded by poxviruses, *Proc. Natl. Acad. Sci. U.S.A. 99*, 6667−6672.
21. Lange, H., Lisowsky, T., Gerber, J., Muhlenhoff, U., Kispal, G., and Lill, R. (2001) An essential function of the mitochondrial sulfhydryl oxidase Erv1p/ALR in the maturation of cytosolic Fe/S proteins, *EMBO Rep. 2*, 715−720.
22. Lu, C., Li, Y., Zhao, Y., Xing, G., Tang, F., Wang, Q., Sun, Y., Wei, H., Yang, X., Wu, C., Chen, J., Guan, K., Zhang, C., Chen, H., and He, F. (2002) Intracrine hepatopoietin potentiates AP-1 activity through JAB1 independent of MAPK pathway, *FASEB J. 16*, 90−92.
23. Polimeno, L., Margiotta, M., Marangi, L., Lisowsky, T., Azzarone, A., Ierardi, E., Frassanito, M. A., Francavilla, R., and Francavilla, A. (2000) Molecular mechanisms of augmenter of liver regeneration as immunoregulator: its effect on interferon-gamma expression in rat liver, *Dig. Liver Dis. 32*, 217−225.
24. Janolino, V. G., and Swaisgood, H. E. (1987) Sulfhydryl oxidase-catalyzed formation of disulfide bonds in reduced ribonuclease, *Arch. Biochem. Biophys. 258*, 265−271.
25. Swaisgood, H., and Janolino, V. (2003) Mammalian sulfhydryl oxidase, *Food Sci. Technol. 122*, 539−546.
26. Janolino, V. G., Sliwkowski, M. X., Swaisgood, H. E., and Horton, H. R. (1978) Catalytic effect of sulfhydryl oxidase on the formation of three-dimensional structure in chymotrypsinogen A, *Arch. Biochem. Biophys. 191*, 269−277.
27. Goldsmith, L. (1987) Sulfhydryl Oxidase from Rat Skin, *Methods Enzymol. 143*, 510−515.
28. Takamori, K., Thorpe, J., and Goldsmith, L. (1980) Skin sulfhydryl oxidase. Purification and some properties, *Biochim. Biophys. Acta 615*, 309−323.
29. Yamada, H., Takamori, K., and Ogawa, H. (1987) Effect of divalent cations and proteases on skin sulfhydryl oxidase activity, *J. Dermatol. 14*, 212−217.
30. Yamada, H., Suga, Y., Takamori, K., and Ogawa, H. (1994) Stoichiometry of the reaction catalyzed by skin sulfhydryl oxidase, *J. Dermatol. 21*, 394−396.
31. Yamada, H., and Ogawa, H. (1996) (Essential trace element and skin diseases), *Nippon Rinsho 54*, 99−105.
32. Yamada, H. (1989) (Localization in skin, activation and reaction mechanisms of skin sulfhydryl oxidase), *Nippon Hifuka Gakkai Zasshi 99*, 861−869.
33. Hashimoto, Y., Suga, Y., Matsuba, S., Mizoguchi, M., Takamori, K., Seitz, J., and Ogawa, H. (2001) Inquiry into the role of skin sulfhydryl oxidase in epidermal disulfide bond formation: implications of the localization and regulation of skin SOx as revealed by TPA, retinoic acid, and UVB radiation, *J. Invest. Dermatol. 117*, 752−754.
34. Matsuba, S., Suga, Y., Ishidoh, K., Hashimoto, Y., Takamori, K., Kominami, E., Wilhelm, B., Seitz, J., and Ogawa, H. (2002) Sulfhydryl oxidase (SOx) from mouse epidermis: molecular cloning, nucleotide sequence, and expression of recombinant protein in the cultured cells, *J. Dermatol. Sci. 30*, 50.
35. Hoober, K. L., and Thorpe, C. (1999) Egg white sulfhydryl oxidase: Kinetic mechanism of the catalysis of disulfide bond formation, *Biochemistry 38*, 3211−3217.
36. Raje, S., Glynn, N., and Thorpe, C. (2002) A continuous fluorescence assay for sulfhydryl oxidase, *Anal. Biochem. 307*, 266−272.
37. Raje, S., and Thorpe, C. (2003) Inter-domain redox communication in flavoenzymes of the quiescin/sulfhydryl oxidase family: role of a thioredoxin domain in disulfide bond formation, *Biochemistry 42*, 4560−4568.
38. Hoober, K. L., and Thorpe, C. (2002) Flavin-dependent sulfhydryl oxidases in protein disulfide bond formation, *Methods Enzymol. 348*, 30−34.
39. Burley, R., and Vadehra, D. (1989) *The Avian Egg: Chemistry and Biology*, John Wiley, New York.
40. Gladyshev, V. N., Jeang, K. T., and Stadtman, T. C. (1996) Selenocysteine, identified as the penultimate C-terminal residue in human T-cell thioredoxin reductase, corresponds to TGA in the human placental gene, *Proc. Natl. Acad. Sci. U.S.A. 93*, 6146−6151.
41. Williams, C. H., Arscott, L. D., Muller, S., Lennon, B. W., Ludwig, M. L., Wang, P. F., Veine, D. M., Becker, K., and Schirmer, R. H. (2000) Thioredoxin reductase: two modes of catalysis have evolved, *Eur. J. Biochem. 267*, 6110−6117.
42. Zhong, L., Arner, E. S., and Holmgren, A. (2000) Structure and mechanism of mammalian thioredoxin reductase: the active site is a redox-active selenolthiol/selenenylsulfide formed from the conserved cysteine-selenocysteine sequence, *Proc. Natl. Acad. Sci. U.S.A. 97*, 5854−5859.
43. Maret, W. (2000) The function of zinc metallothionein: a link between cellular zinc and redox state, *J. Nutr. 130*, 1455S−1458S.

44. Maret, W. (2003) Cellular zinc and redox states converge in the metallothionein/thionein pair, *J. Nutr. 133*, 1460S−1462S.
45. Maret, W., and Vallee, B. L. (1998) Thiolate ligands in metallothionein confer redox activity on zinc clusters, *Proc. Natl. Acad. Sci. U.S.A. 95*, 3478−3482.
46. Maret, W. (1994) Oxidative metal release from metallothionein via zinc-thiol/disulfide interchange, *Proc. Natl. Acad. Sci. U.S.A. 91*, 237−241.
47. Park, J. S., Wang, M., Park, S. J., and Lee, S. H. (1999) Zinc finger of replication protein A, a non-DNA binding element, regulates its DNA binding activity through redox, *J. Biol. Chem. 274*, 29075−29080.
48. Jakob, U., Eser, M., and Bardwell, J. C. (2000) Redox switch of hsp33 has a novel zinc-binding motif, *J. Biol. Chem. 275*, 38302−38310.
49. Jakob, U., Muse, W., Eser, M., and Bardwell, J. C. (1999) Chaperone activity with a redox switch, *Cell 96*, 341−352.
50. Graf, P. C., and Jakob, U. (2002) Redox-regulated molecular chaperones, *Cell. Mol. Life Sci. 59*, 1624−1631.
51. Krezel, A., Lesniak, W., Jezowska-Bojczuk, M., Mlynarz, P., Brasun, J., Kozlowski, H., and Bal, W. (2001) Coordination of heavy metals by dithiothreitol, a commonly used thiol group protectant, *J. Inorg. Biochem. 84*, 77−88.
52. Krezel, A., Latajka, R., Bujacz, G. D., and Bal, W. (2003) Coordination properties of tris(2-carboxyethyl)phosphine, a newly introduced thiol reductant, and its oxide, *Inorg. Chem. 42*, 1994−2003.
53. Gray, W. R. (1993) Disulfide structures of highly bridged peptides: a new strategy for analysis, *Protein Sci. 2*, 1732−1748.
54. Getz, E. B., Xiao, M., Chakrabarty, T., Cooke, R., and Selvin, P. R. (1999) A comparison between the sulfhydryl reductants tris-(2-carboxyethyl)phosphine and dithiothreitol for use in protein biochemistry, *Anal. Biochem. 273*, 73−80.
55. Han, J. C., and Han, G. Y. (1994) A procedure for quantitative determination of tris(2-carboxyethyl)phosphine, an odorless reducing agent more stable and effective than dithiothreitol, *Anal. Biochem. 220*, 5−10.
56. Burns, J. A., Butler, J. C., Moran, J., and Whitesides, G. M. (1991) Selective Reduction of Disulfides by Tris(2-Carboxyethyl)Phosphine, *J. Org. Chem. 56*, 2648−2650.
57. Gibson, Q. H., Swaboda, B. E. P., and Massey, V. J. (1964) Kinetics and mechanism of action of glucose oxidase, *J. Biol. Chem. 239*, 3927−3934.
58. Podlaha, J., and Podlahov, J. (1973) Compounds Structurally Related to Complexone. 1. Tris(Carboxyethyl)Phosphine, *Collect. Czech. Chem. Commun. 38*, 1730−1736.
59. Ralle, M., Lutsenko, S., and Blackburn, N. J. (2003) X-ray absorption spectroscopy of the copper chaperone HAH1 reveals a linear 2-coordinate Cu(I) center capable of adduct formation with exogenous thiols and phosphines, *J. Biol. Chem*. (in press).
60. Williams, C. H., Jr. (1992) in *Chemistry and Biochemistry of Flavoenzymes* (Müller, F., Ed.) pp 121−211, CRC Press, Boca Raton, FL.
61. Massey, V., and Ghisla, S. (1974) Role of charge-transfer interactions in flavoprotein catalysis, *Ann. N.Y. Acad. Sci. 227*, 446−465.
62. Hemmerich, P., and Lauterwein, J. (1972) in *Inorganic Biochemistry* (Eichorn, G., Ed.) pp 1168−1190, Elsevier, Amsterdam.
63. Yu, M., and Fritchie, C. (1975) Interaction of Flavin with Electron-rich Metals, *J. Biol. Chem. 250*, 946−950.
64. Wu, X., Bishopric, N. H., Discher, D. J., Murphy, B. J., and Webster, K. A. (1996) Physical and functional sensitivity of zinc finger transcription factors to redox change, *Mol. Cell. Biol. 16*, 1035−1046.
65. Swaroop, M., Bian, J., Aviram, M., Duan, H., Bisgaier, C. L., Loo, J. A., and Sun, Y. (1999) Expression, purification, and biochemical characterization of SAG, a ring finger redox-sensitive protein, *Free Radical Biol. Med. 27*, 193−202.
66. Baldwin, M. A., and Benz, C. C. (2002) Redox control of zinc finger proteins, *Methods Enzymol. 353*, 54−69.
67. Wang, M., You, J. S., and Lee, S. H. (2001) Role of zinc-finger motif in redox regulation of human replication protein A, *Antioxid. Redox Signaling 3*, 657−669.
68. Knapp, L. T., and Klann, E. (2000) Superoxide-induced stimulation of protein kinase C via thiol modification and modulation of zinc content, *J. Biol. Chem. 275*, 24136−24145.
69. Kurek, I., Kawagoe, Y., Jacob-Wilk, D., Doblin, M., and Delmer, D. (2002) Dimerization of cotton fiber cellulose synthase catalytic subunits occurs via oxidation of the zinc-binding domains, *Proc. Natl. Acad. Sci. U.S.A. 99*, 11109−11114.
70. Jacob, C., Maret, W., and Vallee, B. L. (1998) Control of zinc transfer between thionein, metallothionein, and zinc proteins, *Proc. Natl. Acad. Sci. U.S.A. 95*, 3489−3494.
71. Jiang, L. J., Maret, W., and Vallee, B. L. (1998) The glutathione redox couple modulates zinc transfer from metallothionein to zinc-depleted sorbitol dehydrogenase, *Proc. Natl. Acad. Sci. U.S.A. 95*, 3483−3488.
72. Fabisiak, J. P., Borisenko, G. G., Liu, S. X., Tyurin, V. A., Pitt, B. R., and Kagan, V. E. (2002) Redox sensor function of metallothioneins, *Methods Enzymol. 353*, 268−281.
73. Misaka, E., and Nakanishi, K. (1966) Studies on lipoamide dehydrogenase of bakers' yeast. V. The effects of metal ions and sulfhydryl reagents on the absorption spectrum of the enzyme, *J. Biochem. 60*, 17−26.
74. Misaka, E., and Nakanishi, K. (1966) Studies on lipoamide dehydrogenase of bakers' yeast. IV. Inactivation by metal ions in the presence of $NADH_2$, *J. Biochem. 59*, 545−549.
75. Huang, G. C., and Brady, A. H. (1973) Cobaltous ion complex of reduced lipoamide dehydrogenase, *Biochemistry 12*, 1093−1099.
76. Gazaryan, I. G., Krasnikov, B. F., Ashby, G. A., Thorneley, R. N., Kristal, B. S., and Brown, A. M. (2002) Zinc is a potent inhibitor of thiol oxidoreductase activity and stimulates reactive oxygen species production by lipoamide dehydrogenase, *J. Biol. Chem. 277*, 10064−10072.
77. Yamada, H., Takamori, K., and Ogawa, H. (1987) Localization and some properties of skin sulfhydryl oxidase, *Arch. Dermatol. Res. 279*, 194−197.
78. Yamada, H., Suga, Y., and Takamori, K. (1989) (Reaction mechanism catalyzed by skin sulfhydryl oxidase), *Nippon Hifuka Gakkai Zasshi 99*, 499−502.
79. Park, S., Seo, H., Lee, S., Kim, W., Song, K., and Eun, H. (1992) Purification of sulfhydryl oxidase from human foreskin tissue and immunohistochemical localization, *Seoul J. Med. 33*, 239−246.
80. Jocelyn, P. C. (1972) *Biochemistry of the SH Group*, Academic Press, London.
81. Cavallini, D., Demarco, C., Dupre, S., and Rotilio, G. (1969) Copper Catalyzed Oxidation of Cysteine to Cystine, *Arch. Biochem. Biophys. 130*, 354−361.
82. Kachur, A. V., Koch, C. J., and Biaglow, J. E. (1999) Mechanism of copper-catalyzed autoxidation of cysteine, *Free Radical Res. 31*, 23−34.
83. Turi, G., Harrison, G., Singh, S., and Coppock, D. (2001) The distribution and specificity of expression of Quiescin Q6 (Q6) in human tissues is associated with both endocrine and non-endocrine protein secretion, *Proc. Am. Assoc. Cancer Res. 42*, 74.

BI0301385